

## 점탄성 유체내에서 낙하하는 원통형 미소체의 거동에 관한 실험적 연구

박복춘<sup>†</sup> · 주용기\* · 백병준\*\* · 강영규\*

<sup>†</sup>전북대학교 기계설계학과, \*전북대학교 기계공학과, \*\*전북대학교 정밀기계공학과  
(1992년 1월 7일 접수)

## An Experimental Study on Hydrodynamic Behavior of a Slender Cylinder Falling in a Viscoelastic Fluid

Bockchoon Pak<sup>†</sup>, Yonggi Ju\*, Byungjoon Baek\*\* and Youngkyu Kang\*

<sup>†</sup>Dept. of Mechanical Engineering and Design, \*Dept. of Mechanical Engineering,  
\*\*Dept. of Precision Mechanical Engineering, Chonbuk National University, Chonju, 560-756, Korea  
(Received January 7, 1992)

### 요 약

저속으로 낙하하는 원통형 미소체의 유체역학적 거동에 대하여 점탄성 유체의 비 뉴우튼 성질의 영향에 관해서 연구가 수행되었다. 원통형 미소체의 직경 및 직경에 대한 길이의 비(Aspect Ratio)의 영향에 관해서도 또한 고찰하였으며, 본 실험에서는 뉴우튼 유체로서 99.5%의 글리세린용액과 점탄성 유체로서 1,000 wppm의 polyacrylamide(Separan AP-273) 수용액이 각각 사용되었다.

낙하하는 미소체의 Aspect Ratio가 증가할수록 무차원 최종속도는 뉴우튼 유체 내에서 보다 점탄성 유체 내에서 그 증가속도가 더욱 더 커짐을 보였다. 뉴우튼 유체 내에서 낙하하는 원통형 미소체의 마찰저항 계수는 실험 데이터로부터 계산된 값과 이론치가 비교적 잘 일치하나, 점탄성 유체에 관한 마찰저항 계수는 본 실험의 결과치와 무한히 긴 원통형 미소체에 대한 기존연구의 이론값과는 상당한 차이가 있음을 알 수 있었다. 이는 점탄성 유체 내에서 수직으로 낙하 하는 원통형 미소체의 저항계수가  $k$ (즉, 용기의 직경에 대한 미소체 직경의 비), power-law index, 레이놀즈수 뿐 아니라 aspect ratio를 포함하는 새로운 관계식이 도출되어야 함을 분명히 보여주고 있다.

**Abstract**—The effect of non-Newtonian properties of a viscoelastic fluid on the hydrodynamics of slowly falling circular cylinders was investigated. The effects of diameter and aspect ratio of the cylinders were also studied. A glycerine solution (99.5%) was used for a Newtonian fluid whereas an aqueous solution of 1,000 wppm polyacrylamide (Separan AP-273) was used for the viscoelastic fluid. The increase of a dimensionless terminal velocity with an increasing aspect ratio was much larger in the viscoelastic solution than in the Newtonian solution. The drag coefficients, determined experimentally in the Newtonian fluid, was in a good agreement with the theoretical prediction. For the viscoelastic fluid, the present drag coefficients showed a significant deviation from the earlier analytical predictions which were calculated using infinitely long circular cylinders. The current

<sup>†</sup>To whom all correspondence should be addressed.

study clearly depicts that the drag coefficient of vertically falling cylinders in the viscoelastic fluid should be expressed using a new correlation, which includes the aspect ratio and  $k$  (i. e., the ratio of falling cylinder diameter to container diameter), the power-law index, and the Reynolds number.

**Keywords:** Creeping flow, slender cylinder, viscoelastic fluid, terminal velocity, drag coefficient.

## 1. Introduction

Among the many fluid mechanics problems, one of the most important classes is that involving the motions of small rigid particles, drops, and bubbles in a viscous fluid. The creeping motions of various shapes of rigid and deformable particles in viscous fluids have been studied in order to understand the behavior of such particles both in quiescent and shear flows of Newtonian fluids. Corresponding studies in viscoelastic fluids have been conducted in order to control the migration and orientation of these particles in polymer solutions, polymer melts, suspension, etc. For instance, the orientation distribution of particles induced by the flow field strongly affects certain macroscopic physical properties such as the rheological behavior of the suspension which plays a crucial role during processing [1-3].

Recently, the creeping flow study of these particles in viscoelastic fluids has been initiated as another potential application in the separation of macromolecules using an electrophoresis technique [4]. Thus, it is necessary to better understand the fluid dynamics of a slender solid specimen under a gravity field both in a viscoelastic and in a Newtonian fluid in order that one may get some mechanical insight for the motion of macromolecules under an electrical field.

Therefore, the present study is aimed to investigate moving behavior as well as the effects of length, diameter, and density of a cylinder on the dimensionless terminal velocity and drag coefficient when the cylinder falls slowly in a Newtonian or viscoelastic fluid. Particular emphasis is placed on the case where the ratio of the diameters of the cylinder and reservoir is extremely small, being on the order of 0.03 or less (i.e.,  $k < 0.03$ ).

## 2. Background

Since Stokes [5] in 1851 analyzed the translational motion of a rigid sphere through an unbounded quiescent fluid at zero Reynolds number, numerous investigators have studied the motions of various shapes of particles, drops, and bubbles in Newtonian fluids which have been extensively summarized by Happel and Brenner [6], Clift *et al.* [7], and Leal [8] etc., Among them, the hydrodynamic drag on a circular cylinder of finite length the with the translational direction normal to and parallel to the symmetry axis in an unbounded viscous fluid reported by Cox [9], can be given as follows, respectively.

$$F' = \frac{4\pi\mu U}{\ln(l/d) + 0.886297} \quad (1a)$$

$$F = \frac{2\pi\mu U}{\ln(l/d) - 0.11370} \quad (1b)$$

where  $l$  and  $d$  are the length and diameter of the cylinder, and  $U$  is the terminal velocity. From this analytical solution, one can find an expression of the drag coefficients for each motion:

$$C'_D = \frac{8\pi}{\ln(l/d) + 0.886297} \frac{1}{\text{Re}} \quad (2a)$$

$$C_D = \frac{4}{\ln(l/d) - 0.11370} \frac{1}{\text{Re}} \quad (2b)$$

Note that the definitions of the drag coefficient are given as:

$$C'_D = \frac{F'/dl}{\frac{1}{2}\rho U^2} \quad (3a)$$

$$C_D = \frac{F/\pi dl}{\frac{1}{2}\rho U^2} \quad (3b)$$

It should be mentioned that conventional definition of the drag coefficient, i.e., based in the projected area of a cylinder, was used for the transverse motion, while that based on the surface area was used for the axial motion in order to compare the current results with the other theoretical predictions.

Manero *et al.* [10] investigated the axial motion, sometimes called the vertical motion in a gravitational field, of an infinitely long rod (i.e., when the aspect ratio, AR, is infinity) inside a cylinder theoretically and experimentally. The following correlation was suggested for the motion in a Newtonian fluid.

$$C_D = \frac{-4}{1 + \frac{1+k^2}{1-k^2}} \frac{1}{\ln k} \quad (4)$$

Leal [11] theoretically investigated the creeping motion of slender, axisymmetric rod-like particles using a perturbation expansion for rheologically slow flow. In the appendix of his paper, Leal and Zana reported their preliminary experimental observations on the motion of cylindrical rods (aspect ratios of 28 and 66) falling in a quiescent fluid. Glycerine (99.5%), a Newtonian fluid, and 0.5% aqueous solution of polyacrylamide (Separan AP-30), a viscoelastic fluid, were used as test fluids. In the Newtonian fluid, the orientation of the cylinder was fully determined by the initial orientation, provided that the cylinder did not drift too close to the side wall of the reservoir tank. No intrinsic preference was shown for any orientation. In contrast, in the Separan solution, the cylinder was found to rotate rapidly from its initial orientation to a vertical one which was completely independent of the initial orientation. Thus, Leal and Zana concluded that the non-Newtonian characteristics of the ambient fluid caused intrinsically preferred equilibrium orientations.

Chiba *et al.* [12] experimentally demonstrated that a cylinder falling in Newtonian liquids rotated to adopt a horizontal orientation, whereas in non-Newtonian liquids (i.e., aqueous solutions of polyacrylamide and hydroxyethyl cellulose), the body rotated towards a vertical orientation. In addition,

the time-dependent reorientation behavior of the cylinder was studied at different concentrations of viscoelastic liquids and was explained by relating to the shear-thinning characteristics and elasticity of the viscoelastic fluids. However, the falling behavior of the cylinder in these viscoelastic liquids after it reached the steady terminal state was not investigated.

Manero *et al.* [6] investigated the axial motion of a cylinder being pulled along the center of a cylindrical container. They proposed the following correlation for the drag coefficient of the cylinder moving in a non-Newtonian fluid:

$$C_D = \frac{C(n)}{Re} \quad (5)$$

where  $C(n)$  was given as  $4(1-n)/n$  for the limiting case of  $k \rightarrow 0$ , assuming that no pressure gradient was generated by the motion of the cylinder.

They also found that when Manero *et al.* took into account the effect of the induced pressure gradient due to the presence of the reservoir wall,  $C(n)$  became substantially greater than in the case with no pressure gradient. Considering the wall effect, the induced pressure gradients were much greater for a Newtonian fluid than for a viscoelastic fluid. In the latter case, the induced pressure gradients were considered to be negligibly small when the diameter of falling cylinder was small compared to the reservoir diameter. For the viscoelastic liquid, the drag coefficient,  $C_D$ , was found to follow an asymptotic limiting solution, Eq. (5), obtained from a simple inelastic analysis, provided  $k < 0.02$ .

### 3. Experimental Methods

Large aspect-ratio cylindrical slender bodies were made of aluminum rod with 0.125 mm diameter and hollow glass tubes of various diameters with metal inserts. Especially, a dummy weight was inserted in the front part of the hollow glass tube to make it fall vertically in a Newtonian fluid. The length varied from 1.2 to 310.8 mm, resulting in the aspect ratios (AR) of 10 to 830. The densities of the aluminum and the hollow glass cylin-

ders with metal inserts were 2.852 and 2.700  $\text{g}/\text{cm}^3$ , respectively.

A 99.5% glycerine (Fisher Scientific Co., U.S.A.) was chosen as a test fluid to represent the hydrodynamic behavior of these large aspect-ratio cylinders in a Newtonian fluid. An aqueous solution of polyacrylamide (Separan AP-273) with the concentration of 1000 wppm was chosen to investigate falling motions of these cylinders in a viscoelastic fluid.

Two different types of reservoirs (i.e., rectangular and cylindrical ones) were used for the experiments. The former with a rectangular base 90 cm by 14.3 cm was to observe the falling behavior of a slender cylinder in Newtonian and viscoelastic fluids, and the latter was to measure the terminal velocities of a cylinder falling vertically in a viscoelastic fluid. Four different cylindrical test chambers were used with their inside diameters of 6.0, 10.05, 13.21, and 14.3 cm. Thus, the ratios of the diameter of the cylinder to that of the reservoir ( $k$ ) ranged from 0.00087 to 0.0483. The wall effect of cylinders on the terminal velocity were checked from the four different size reservoirs. The heights of all reservoirs were 1 m.

Special launching devices that helped to introduce the slender cylinders into the reservoir horizontally or vertically were utilized. Horizontal lines were marked for every 10 cm distance for each reservoir in order to measure terminal velocities. The terminal velocity was calculated by dividing the interval between two pre-marked lines i.e., 40 and 60 cm respectively from the top of a reservoir, by the time taken for the cylinder to pass the lines. Experiments were repeated twice for each cylinder, and the final result was based on the averaged data. The deviation between the two runs were less than 5 percent.

A plot of the drag coefficient versus the Reynolds number was made to compare the experimental data with available analytical data in the literature for the Newtonian fluid. The drag coefficient was calculated from Eq. (3). The viscosity of the polyacrylamide solution varies so significantly that it became a major task to find the corresponding viscosity to a given terminal velocity. The Reyno-

lds number for the polyacrylamide solution was calculated by using the apparent viscosity corresponding to the terminal velocity. Detailed procedures to calculate the local shear rate and the apparent viscosity are given in the following section.

## 4. Results and Discussion

### 4.1. Viscosities of the test fluids

The viscosity results of the glycerine and the aqueous solution of 1,000 wppm polyacrylamide are shown in Fig. 1. The viscosity of glycerine is 852.2 (mPa·s). The polyacrylamide 1,000 wppm solution shows a typical shear-thinning behavior, i.e., the apparent viscosity decreases as the shear rate increases. Since the apparent viscosity is used to calculate the Reynolds number,  $Re$ , the relationship between the shear rate and apparent viscosity for the polyacrylamide solution is obtained from the experimental data in Fig. 1 by the least squares curve-fitting technique:

$$\log(\eta) = 3.08235 \times 10^{-2} (\log \dot{\gamma})^3 + 1.24891 \times 10^{-2} (\log \dot{\gamma})^2 - 7.09994 \times 10^{-1} \log \dot{\gamma} - 2.81116 \times 10^{-1} \quad (6)$$

$(0.00288 \text{ s}^{-1} \leq \dot{\gamma} \leq 255.105 \text{ s}^{-1})$

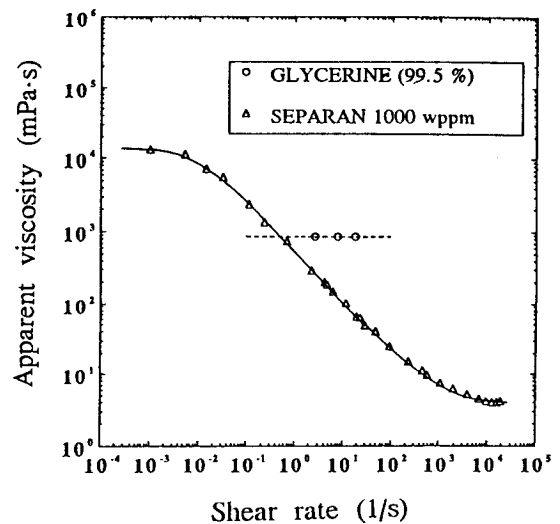


Fig. 1. Viscosity vs. shear rate curve of glycerine and polyacrylamide (Separan AP-273) solutions measured at 25°C.

In the intermediate region of the shear rate, the polyacrylamide solution shows a power-law type behavior as expected. The flow index,  $n$ , is determined to be 0.419 in that region, which is then used to compare present drag coefficient data with those values calculated by Manero *et al.* [10].

**4.2. Falling behavior**

The falling behavior of a slender cylinder was observed in a rectangular reservoir with a glycerine and an aqueous solution of 1,000 wppm polyacrylamide respectively. It was demonstrated that a slender cylinder of 5 cm in length falling in the Newtonian fluid rotates to adopt a horizontal orientation, whereas in the viscoelastic fluid it rotates towards the vertical orientation as Leal [11] and Chiba *et al.* [12] observed. However, for very dilute solutions of polyacrylamide it was not able to reach the vertical orientation and moved sideways with a constant orientation angle regardless of an initial orientation as shown in Fig. 2. Fig. 3 shows the concentration effect on the constant orientation angle of a cylinder falling in very dilute solutions of polyacrylamide. As the concentration increases the orientation angle of a falling cylinder decreases. It means that a slender cylinder

increasingly attempts to fall vertically as the concentration increases, and eventually falls vertically in the solutions of a 200 wppm and higher concentrations.

**4.3. Terminal velocity**

After a falling cylinder reaches its final orientation in the fluids, the velocity remains constant, so called the terminal velocity, due to the force balance between gravitational and buoyancy forces acting on a falling object. The effect of the aspect-ratio on the terminal velocity is examined for both the glycerine and the polyacrylamide solution. Since a cylinder falls horizontally in a Newtonian fluid regardless of its initial orientation as aforementioned, the terminal velocity is measured by dropping a cylinder with horizontal position initially in a rectangular reservoir. Fig. 4 indicates the effect of the aspect-ratio on the dimensionless terminal velocity of a cylinder falling horizontally in the glycerine for  $k=0.00087$  and  $\rho_s=2.852 \text{ g/cm}^3$ . Here  $k$  is defined as the ratio of the diameter of a slender cylinder to the width of a rectangular reservoir. The dimensionless terminal velocity,  $U^+$ , is obtained by dividing the measured terminal velocity by the terminal velocity of the cylinder with the aspect ratio of  $AR=10$ . As shown in the

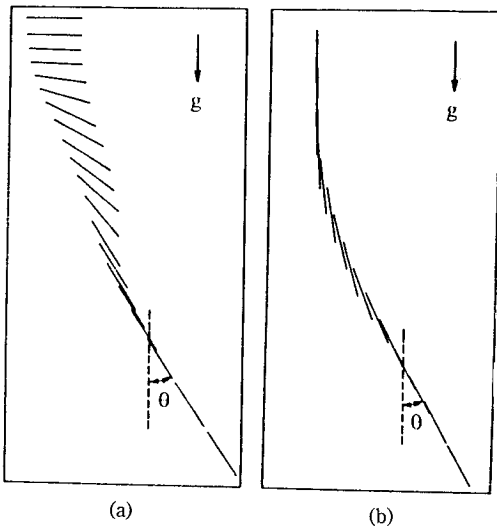


Fig. 2. Falling behavior of a slender cylinder in very dilute polyacrylamide solutions.  
 (a) Initially horizontal orientation  
 (b) Initially vertical orientation

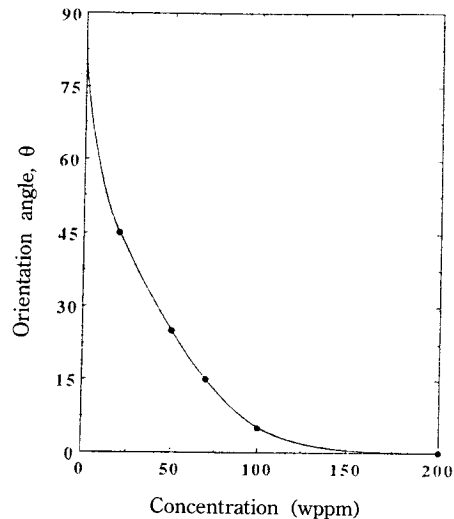


Fig. 3. The concentration effect of polyacrylamide solutions on the orientation angle of a falling cylinder.

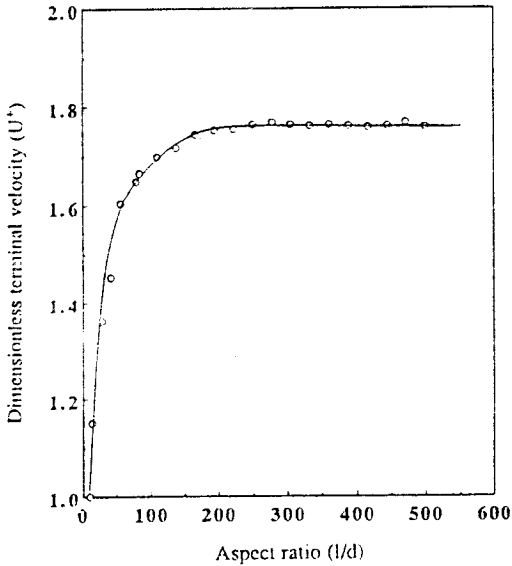


Fig. 4. Dimensionless terminal velocity ( $U^+$ ) vs. aspect ratio ( $l/d$ ) with cylinders of  $k=0.00087$  and  $\rho_s=2.852 \text{ g/cm}^3$  falling horizontally in glycerine inside a rectangular reservoir.

figure the dimensionless terminal velocity increases with increasing the aspect ratio of a cylinder, however, it reaches the asymptotic value of 1.8 at the aspect ratio of 200. It implies that the drag force per unit length remains constant for the longer cylinder than that of the aspect ratio of 200.

Fig. 5 shows the dimensionless terminal velocity,  $U^+$ , of hollow glass cylinders ( $k=0.00537$  and  $\rho_s=2.70 \text{ g/cm}^3$ ) falling vertically in the glycerine and the polyacrylamide solution. Note that the data shown in open square symbols are obtained from the glycerine while the data shown in open circle symbols are obtained from the polyacrylamide solutions. As shown in the figure, the effect of the aspect ratio on the dimensionless terminal velocity is quite different between the glycerine and the polyacrylamide solutions. When the aspect ratio is changed from 10 to 130, the value of  $U^+$  is approximately doubled for the glycerine while it is increased by 4.5 times for the polyacrylamide solution. Similar trends are observed in the tests with different  $k$  values which are not shown here.

The effect of the cylinder diameter on the dimensionless terminal velocity, sometimes called

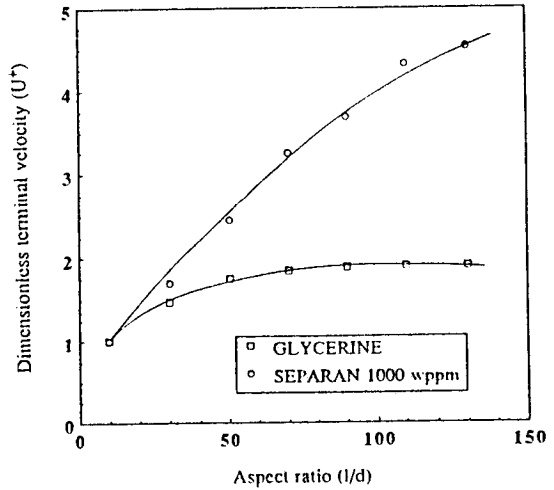


Fig. 5. Dimensionless terminal velocity ( $U^+$ ) vs. aspect ratio ( $l/d$ ) with cylinders of  $k=0.00537$  and  $\rho_s=2.70 \text{ g/cm}^3$  falling vertically in a cylindrical reservoir.

the wall effect, is studied in the glycerine and the polyacrylamide solution and is shown in Figs. 6(a) and 6(b). The nominal density of hollow glass cylinders used is  $2.70 \text{ g/cm}^3$ . As shown in Fig. 6(a), the increase in the terminal velocity of the cylinder in the glycerine with an increasing aspect ratio is greater for the cylinder with a smaller diameter than for the cylinder with a larger one. In contrast, the reverse trend is observed in the polyacrylamide solution as depicted in Fig. 6(b). As shown in Fig. 6(b), the asymptotic value of  $U^+$  in the Separan solution is approximately 2.0 for the smallest value of  $k$  (i.e.,  $k=0.00087$ ) whereas the value of  $U^+$  reaches 4.6 for the largest  $k$  value case (i.e.,  $k=0.01219$ ) and still increases as the aspect ratio increases.

#### 4.4. Drag coefficients

When a circular cylinder falls slowly and reaches the steady-state terminal motion, the force balance acting on the cylinder can be expressed as follows.

$$F = F_g - F_b \quad (7)$$

where  $F$  is the total drag force,  $F_g$  the gravity force ( $=\rho_s Vg$ ), and  $F_b$  the buoyancy force ( $=\rho_f Vg$ ),

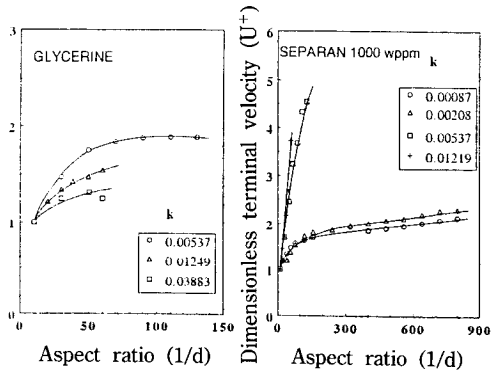


Fig. 6. (a) and (b) Dimensionless terminal velocity ( $U^+$ ) vs. aspect ratio ( $l/d$ ) with cylinders of different diameters ( $\rho_s = 2.70 \text{ g/cm}^3$ ) falling vertically in a cylindrical reservoir.

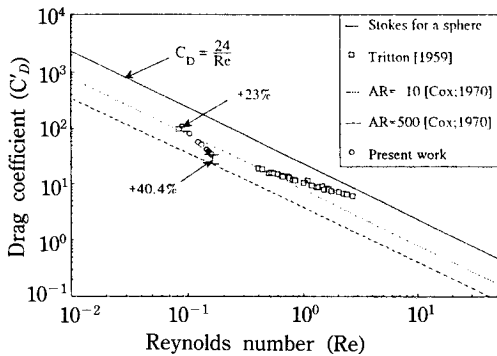


Fig. 7. Drag coefficient ( $C'_D$ ) vs. Reynolds number for aluminium cylinders falling horizontally in glycerine ( $\rho_s = 2.852 \text{ g/cm}^3$  and  $k = 0.00087$ ).

respectively.

Once the total drag force is calculated, the drag coefficients from experimental data may be obtained with equation (3).

Fig. 7 shows the drag coefficients for circular cylinders (aspect ratio=10 to 500) falling horizontally in glycerine inside a rectangular reservoir. The theoretical predictions by Cox [9] and the previous experimental results by Tritton [13] are together indicated for comparison. Note that Cox's predictions were obtained for a cylinder falling horizontally in an unbounded fluid medium (i.e.,  $k=0$ ), and Tritton's data the drag coefficients for the flow across a circular cylinder ( $k=0$  and  $AR=\infty$ ). As shown in the figure, the drag coeffi-

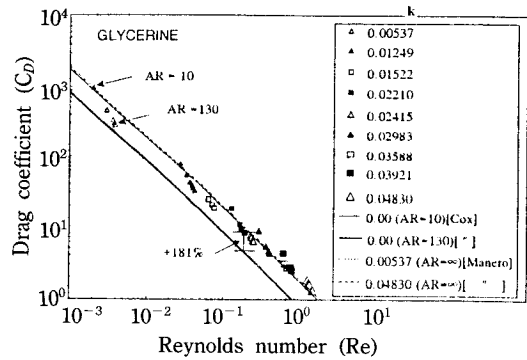


Fig. 8. Drag coefficient ( $C_D$ ) vs. Reynolds number for the cylinders falling vertically in glycerine ( $\rho_s = 2.70 \text{ g/cm}^3$ ).

cients for the cylinders of aspect ratios of 10 and 500 are approximately 23% and 40.4% larger than those by Cox's predictions respectively, which may be attributed to the wall effect for the current experimental data.

The drag coefficients obtained with circular cylinders with aspect ratios from 10 to 130, falling vertically in glycerine, are presented in Fig. 8. The predictions by Cox [9] and Manero *et al.* [10] are also given for comparison. Note that Cox's correlation was obtained for a cylinder falling in an unbounded fluid medium, i.e.,  $k=0$  whereas Manero *et al.*'s correlation was derived for an infinitely long cylinder, i.e.,  $AR=\infty$ . The drag coefficients predicted by Cox for  $k=0$  and  $AR=130$  correlate with those calculated by Manero *et al.* for  $k=0.00537$  and  $AR=\infty$ . The present experimental results of the drag coefficient,  $C_D$ , for the smallest cylinder diameter (i.e.,  $k=0.00537$ ) and the largest aspect ratio (i.e.,  $AR=130$ ) correlate with the predicted values of Cox and Manero *et al.* As the value of  $k$  increases from 0.00537 to 0.0483, the drag coefficient data begin to deviate from the predicted values by Cox and Manero *et al.* For example, the large triangle and square symbols (i.e.,  $k>0.02$ ) as indicated in Fig. 8 are off by almost 181%.

The cause of this deviation of the current drag coefficient data from the two aforementioned correlations is explained as follows: The current experimental  $C_D$  data contains the effects of wall

boundary and aspect ratio. In addition, the current data at a high Reynolds number (i.e.,  $Re > 1$ ) may reflect some inertia effect. Cox's correlation does not include the wall effect whereas Manero *et al.*'s correlation does not include the effect of aspect ratio. Both Cox and Manero *et al.* did not consider the inertia terms when deriving their correlations of the drag coefficient. Note that it is not clear what the threshold Reynolds number is, below which the inertia effect can be neglected. In short, neither Cox nor Manero *et al.* accurately predicts the drag coefficient of a finite length cylinder falling in a Newtonian fluid bounded by a wall. Clearly, there should be a new correlation for the Newtonian fluid that combines the aspect ratio (AR), the ratio of the cylinder diameter to container diameter ( $k$ ), and  $Re$ .

Fig. 9(a) and 9(b) present drag coefficients of the circular cylinders having aspect ratios from 10 to 830, falling vertically in the 1,000 wppm polyacrylamide solution. The predictions by Manero *et al.* [10] for different  $k$  values are also shown for comparison. Before discussing the current results, the procedure to calculate the Reynolds number,  $Re$ , is briefly described next.

The calculation of the Reynolds number requires the apparent viscosity which varies with the shear rate for the viscoelastic solution. The shear rate depends on a terminal velocity, which subsequently depends on the densities of cylinder and solution. Hence, the apparent viscosity corresponding to each test run should be calculated using some analytical solution. Manero *et al.* [10] gave an explicit expression of the wall shear stress at the surface of the cylinder from which one can obtain the wall shear rate expression for a power-law fluid as:

$$\left[ \frac{du}{dr} \right]_w = \left( \frac{1-n}{n} \right) \frac{2U}{d} \frac{1}{1-k \frac{1-n}{n}} \quad (8)$$

Note that this equation could be reduced to a simpler form when  $k$  is very small. The wall shear rate corresponding to a particular terminal velocity is determined using Eq. (8), and the apparent viscosity is determined from the viscosity curve given by Eq. (6). The range of the wall shear rate

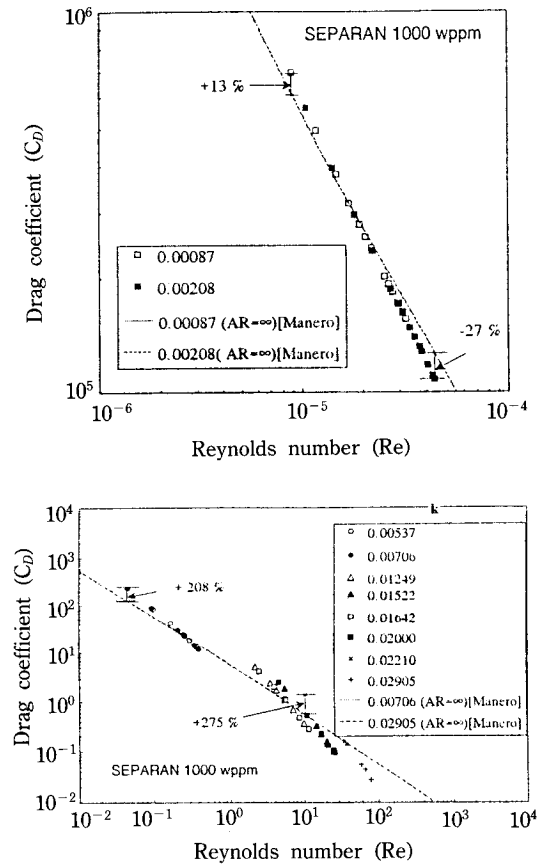


Fig. 9. (a) Drag coefficient ( $C_D$ ) vs. Reynolds number in a polyacrylamide Separan solution for small  $k$  value cases (i.e.,  $k < 0.0021$ ). The densities of all cylinders are  $\rho_s = 2.852 \text{ g/cm}^3$ , (b) Drag coefficient ( $C_D$ ) vs. Reynolds number in a polyacrylamide Separan solution for large  $k$  value cases (i.e.,  $k < 0.005$ ). The densities of all cylinders are  $2.70 \text{ g/cm}^3$ .

for the polyacrylamide solution is from 0.7 to  $894 \text{ s}^{-1}$ .

Fig. 9(a) shows the drag coefficient data,  $C_D$ , for relatively small diameter cylinder cases (i.e.,  $k \leq 0.002$ ) with a Reynolds number less than  $10^{-4}$ . In this figure, the Reynolds number,  $Re$ , varies from  $9 \times 10^{-6}$  to  $4.2 \times 10^{-5}$  when the aspect ratio is varied from 10 to 830. The predicted drag coefficients by Manero *et al.* [10] (i.e., see dotted and dashed lines), in general, correlate well with the current experimental data for the cases of small  $k$  values.



However, since the Manero *et al.* correlation does not consider the effect of aspect ratio, the slope in the  $C_D$  vs.  $Re$  curve differs from that of Manero *et al.*, meaning that the discrepancy is largest for the shortest and longest cylinders with cylinders of a fixed diameter. For example, the current experimental value of  $C_D$  for an aspect ratio of 10 and  $k=0.00087$  (the shortest one among the smallest diameter cylinders in the current study) is 13 percent greater than the Manero *et al.* data whereas the value for an aspect ratio of 830 and  $k=0.00087$  (the longest one among the smallest diameter cylinders) is 27 percent smaller than the Manero *et al.* data.

Fig. 9(b) shows the drag coefficient data,  $C_D$ , for relatively large diameter cylinder cases (i.e.,  $k \geq 0.002$ ) with a Reynolds number greater than  $10^{-2}$ . The current  $C_D$  data for relatively large  $k$  value cases deviate significantly from the predicted drag coefficients by Manero *et al.* [10]. For example, the experimental drag coefficient shown in a small open square symbol with the Reynolds number of 0.045 is 208 percent greater than the predicted value by Eq. (5), whereas the datum shown in a large square symbol with the Reynolds number of 10 is 275 percent larger than the one calculated by Eq. (5). This discrepancy shows the limitations of the predictions of Manero *et al.*, Eq. (5).

As the Reynolds number increases greater than 1, one may think that the effect of the inertia force may be increasingly important. However, the comparison between the current experimental drag coefficient data and those predictions from Eq. (5) indicates that the inertia effect is relatively small even at the Reynolds number of 100 for the cases of  $k \leq 0.03$ . The reason being that if inertia force plays a significant role, experimental drag coefficient should have been greater than the predicted value by Eq. (5), not smaller.

Therefore, it is believed that the elasticity of the polyacrylamide solution [14] plays a significant role in reducing the total drag of large aspect-ratio cylinders. This is manifested by an increase in the dimensionless terminal velocity for the polyacrylamide solution as shown in Figs. 4

and 5b. The increase in the dimensionless terminal velocity is equivalent to a drag reduction, caused by the decrease in the apparent viscosity near the wall of a falling cylinder. In other words, the reduction of an apparent viscosity may be related to structural changes of polyacrylamide molecules in the aqueous solution near the falling cylinder. To our best knowledge, this type of drag reduction has not been reported in the literature before.

The current experimental study suggests that the drag coefficient,  $C_D$ , of a slowly falling cylinder in a non-Newtonian fluid bounded by a wall is a function of the aspect ratio (AR), the ratio of the cylinder diameter to container diameter ( $k$ ), the power-law index ( $n$ ), and the Reynolds number ( $Re_d$ ):

$$C_D = f(Re, AR, k, n) \quad (9)$$

## 5. Summary and Conclusions

The effects of the viscoelasticity of the polyacrylamide solution, the aspect-ratio, and the diameter of cylinders has been examined to investigate the hydrodynamic behavior of circular cylinders. Terminal velocity measurements with circular cylinders in various diameters and lengths have been conducted in a glycerine (a Newtonian fluid) and a polyacrylamide solution (a viscoelastic solution). The results can be summarized as follows:

1) The dimensionless terminal velocity of a slender cylinder falling in the viscoelastic fluid varies much greater than in the Newtonian fluid as the aspect-ratio is increased.

2) The diameter effect on the dimensionless terminal velocity for the viscoelastic solution is found to be the opposite of the trend observed in the Newtonian fluid.

3) The current drag coefficient data in the Newtonian fluid correlate with the predicted values of Cox and Manero *et al.* for the smallest cylinder diameter (i.e.,  $k=0.00537$ ) and the largest aspect ratio (i.e.,  $AR=130$ ). As the value of  $k$  increases from 0.00537 to 0.0483, the drag coefficient data begin to deviate from the predicted values by Cox and Manero *et al.*

4) The drag coefficient data in the viscoelastic solution for relatively small cylinder diameter cases (i.e.,  $k \leq 0.002$ ) with a Reynolds number less than  $10^{-4}$  are, in general, in a fair agreement with the predicted drag coefficients by Manero *et al.* For relatively large diameter cylinder cases (i.e.,  $k \geq 0.002$ ) with a Reynolds number greater than  $10^{-2}$ , the current  $C_D$  data significantly deviate from the predicted drag coefficients by Manero *et al.*

### Acknowledgement

The authors express their appreciation to the Korea Research Foundation for financial support and special thanks to professor Young I. Cho of Drexel University, U.S.A. for his valuable advice.

### Nomenclatures

AR : aspect ratio ( $=l/d$ ); dimensionless  
 $C_D'$  : drag coefficient, defined as the equation (2a)  
 $C_D$  : drag coefficient, defined as the equation (2b)  
 $d$  : diameter of a slender cylinder  
 $F'$  : drag force, defined as the equation (1a)  
 $F$  : drag force, defined as the equation (1b)  
 $g$  : gravitational acceleration  
 $k$  : ratio of the diameter of cylindrical body to the diameter of reservoir, dimensionless  
 $l$  : length of cylinder  
 $n$  : power-law index  
 $Re$  : Reynolds number based on cylinder diameter  
 $U$  : terminal velocity  
 $U^+$  : dimensionless terminal velocity ( $=U/U_{AR=10}$ )  
 $V$  : volume of slender cylinder

$\dot{\gamma}$  : shear rate ( $s^{-1}$ )  
 $\eta$  : apparent viscosity of non-Newtonian fluid  
 $\mu$  : viscosity of Newtonian fluid  
 $\rho_f$  : density of fluid  
 $\rho_s$  : density of slender cylinder

### References

1. M.W. Darlinton and P.L. McGinley, *J. Material Science, Letters*, **10**, 906 (1975).
2. R.C. Gilver, M.J. Crochet and R. B. Pipes, *J. Comp. Materials*, **17**, 330 (1983).
3. S. Goto, H. Nagazono and H. Kato, *Rheol. Acta*, **25**, 119 (1986).
4. Insik Kim and Young I. Cho, *J. Non-Newtonian Fluid Mech.*, **33**, 219 (1989).
5. G.G. Stokes, *Trans. Cambridge Phil. Soc.*, **9**, 8 (1851).
6. J. Happel and H. Brenner, "Low Reynolds number hydrodynamics", Kluwer Academic Publishers, Dordrecht, The Netherlands (1965).
7. R. Clift, J.R. Grace and M.E. Weber, "Bubble, Drops, and Particles", Academic Press, A Subsidiary of Harcourt Brace-Jovanovich, Publishers (1978).
8. L.G. Leal, *Annual Review of Fluid Mechanics*, **12**, 435 (1980).
9. R.G. Cox, *J. Fluid Mech.*, **44**, 791 (1970).
10. A. Manero, B. Mena and L. De Vargis, *Rheol. Acta*, **26**, 266 (1987).
11. L.G. Leal, *J. Fluid Mech.*, **69**, 305 (1975).
12. K. Chiba, Ki-Won Song and A. Horikawa, *Rheol. Acta*, **25**, 360 (1986).
13. D.J. Tritton, *J. Fluid Mech.*, **6**, 547 (1959).
14. A. Argumedo, T.T. Tung and K.I. Chang, *J. Rheology*, **22**, 449 (1978).